Journal of Organometallic Chemistry, 466 (1994) 185–199

The reaction of iron pentacarbonyl with 6-aminofulvenes: some organic chemistry of *R,S* and *R,R/R,S*-$[Fe_2\{\eta,\eta\text{-}C_5H_4CH(NMe_2)CH(NMe_2)C_5H_4\}(CO)_2(\mu\text{-}CO)_2]$

Brian Callan, M. Gary Cox, Anita McCabe, A.R. Manning, Pardeep Sayal, Paul Soye and Stephen C. Wade

Department of Chemistry, University College, Belfield, Dublin 4 (Ireland)

F.S. Stephens

School of Chemistry, Macquarie University, North Ryde, N.S.W. 2109 (Australia)

P. McArdle and D. Cunningham

Department of Chemistry, University College, Galway (Ireland)

(Received April 22, 1993)

Abstract

Iron pentacarbonyl reacts with 6-dimethylaminofulvene in refluxing xylene to give three products, **1**, **2** and **3**. Compound **1** is *R,S*-$[Fe_2\{\eta,\eta\text{-}C_5H_4CH(NMe_2)CH(NMe_2)C_5H_4\}(CO)_2(\mu\text{-}CO)_2]$, **2** is its *R,R/S,S* isomer, and **3** is $[Fe_2\{\eta^3,\eta^5\text{-}Me_2NCHC_5H_3CH\text{-}C_5H_4\}(CO)_5]$. Compound **3** is favoured by high reactant concentrations and an excess of $[Fe(CO)_5]$. Analogues of **2** and **3** but not **1** may be prepared by using 6-Me(Ph)$NCHC_5H_4$, 6-$Et_2NCHC_5H_4$ and 6-${}^iPr_2NCHC_5H_4$; the last of these also gives the unlinked dimer $[Fe\{\eta^5\text{-}C_5H_4CH_2N^iPr_2\}_2(CO)_2(\mu\text{-}CO)_2]$. This behaviour is attributed to the steric effects of the NR_2 groups on the formation of the ring-linking C–C bond. Dynamic NMR studies show that in **1**, but not **2**, there is a slowable restricted rotation about this bond and, in both **1** and **2**, rotation–inversion about the nitrogen atoms of the NMe_2 groups can be slowed. Compounds **1** and **2** are derivatives of a 1,2-bis-dimethylaminoethane, and as such have an extensive organic chemistry that leaves the $Fe_2(CO)_2(\mu\text{-}CO)_2$ moieties intact. There are differences between **1** and **2**, due to conventional stereochemical effects, and consequently the $Fe_2(CO)_2(\mu\text{-}CO)_2$ fragments are involved in some instances; this leads to unexpected and unusual reactions. The structures of **2** and the ketone $[Fe_2\{\eta,\eta\text{-}C_5H_4CH_2C(O)C_5H_4\}(CO)_2(\mu\text{-}CO)_2]$ have been confirmed by X-ray diffraction studies and are compared with that previously reported for **1**.

Key words: Iron; Carbonyl; Fulvene; Chirality

1. Introduction

6-Dimethylaminofulvene reacts with $[Fe(CO)_5]$ to give two isomers of $[Fe_2\{\eta,\eta\text{-}C_5H_4CH(NMe_2)CH(NMe_2)C_5H_4\}(CO)_2(\mu\text{-}CO)_2]$ (**1** and **2**) [1]. Both are derivatives of the well-known $[Fe_2(\eta\text{-}C_5H_5)_2(CO)_2(\mu\text{-}CO)_2]$ constrained to a *cis* configuration by the $-CH(NMe_2)CH(NMe_2)-$ moiety linking their cyclopentadienyl ligands. The two linking carbon atoms are chiral. An X-ray diffraction study subsequently showed that **1** is the *meso* or *R,S* isomer [2]. The present work has confirmed that **2** is one of the two possible *R,R/S,S* or racemic isomers, and that under certain conditions a third product is formed at the expense of **1** and **2**. This is $[Fe_2(C_{14}H_{11}N)(CO)_5]$ (**3**) which was previously obtained with a very low yield from the reaction of 6-dimethylaminofulvene with $[Fe_2(CO)_9]$ at room temperature [3]. The structures of **1**–**3** are shown in Fig. 1.

Compounds **1** and **2** have an extensive organic chemistry that leaves the $[Fe_2(CO)_2(\mu\text{-}CO)_2]$ moiety unchanged provided that care is taken in the selection

---

Correspondence to: Dr. A.R. Manning.

0022-328X/94/\$7.00
SSDI 0022-328X(93)23981-3

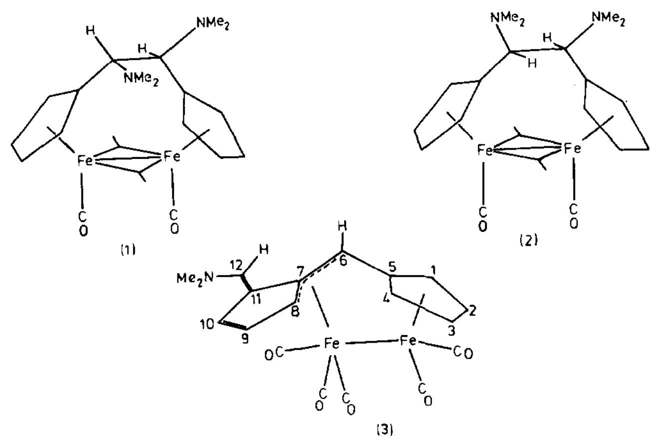

Fig. 1. The structures of **1**, **2** and **3**. μ-CO groups have been omitted from **1** and **2**. Atom numbering on **3** is taken from ref. 3.

of reagents. A preliminary report of this work has appeared [4].

2. Experimental details

Published methods or extensions thereof were used to prepare 6-dimethylaminofulvene, 6-diethylaminofulvene, 6-di-isopropylaminofulvene and 6-methylphenylaminofulvene [5]. Other chemicals were purchased.

All reactions were carried out at room temperature in dried and deoxygenated solvents under nitrogen unless otherwise stated. Hexane, benzene, toluene, xylene, acetonitrile, tetrahydrofuran and dichloromethane were dried by refluxing over calcium hydride and distilled prior to use. Tetrahydrofuran was further distilled from sodium–benzophenone and $LiAlH_4$ if required.

Infrared spectra were run on a Perkin–Elmer 1710 FTIR spectrometer. NMR spectra were run on a JEOL JNM-GX 270 FT NMR spectrometer with Me_4Si as an internal standard.

Analyses were carried out in the Analytical Laboratory, University College, Dublin.

2.1. *Reaction of 6-aminofulvenes ($C_5H_4CHNR_2$) with $[Fe(CO)_5]$*

A solution of 6-dimethylaminofulvene (6 g, 50 mmol) and $[Fe(CO)_5]$ (14.6 g, 74.5 mmol) in xylene (70 cm^3) was refluxed for 2 h. Solvent removal and chromatography on alumina gave three products: $[Fe(\eta^3,\eta^5\text{-}Me_2NCHC_5H_3CHC_5H_4)(CO)_5]$ (**3**) eluted with hexane and recrystallized from toluene–pentane mixtures as brown–purple crystals; R,S-$[Fe_2\{\eta,\eta\text{-}C_5H_4CH(NMe_2)CH(NMe_2)C_5H_4\}(CO)_2(\mu\text{-}CO)_2]$ (**1**) eluted with benzene and recrystallized from toluene–dichloromethane mixtures as purple crystals; red $R,R/S,S$-$[Fe_2\{\eta,\eta\text{-}C_5H_4CH(NMe_2)CH(NMe_2)C_5H_4\}(CO)_2(\mu\text{-}CO)_2]$ (**2**) eluted with acetone and crystallized from it.

Under the same conditions, other aminofulvenes gave a mixture of analogues of **2** and **3**: $C_5H_4CHNEt_2$ gave $[Fe_2\{\eta,\eta\text{-}C_5H_4CH(NEt_2)CH(NEt_2)C_5H_4\}(CO)_2(\mu\text{-}CO)_2]$ (**2a**) (41% yield) and $[Fe(\eta^3,\eta^5\text{-}Et_2NCHC_5H_3CHC_5H_4)(CO)_5]$ (**3a**) (43% yield); $C_5H_4CHN\text{-}{}^iPr_2$ gave $[Fe_2\{\eta,\eta\text{-}C_5H_4CH(N^iPr_2)CH(N^iPr_2)C_5H_4\}(CO)_2(\mu\text{-}CO)_2]$ (**2b**), (23% yield) and $[Fe(\eta^3,\eta^5\text{-}{}^iPr_2NCHC_5H_3CHC_5H_4)(CO)_5]$ (**3b**) (10% yield) as well as $[Fe_2(\eta^5\text{-}C_5H_4CH_2N^iPr_2)_2(CO)_4]$ (15% yield); $C_5H_4CHN(Me)Ph$ gave only $[Fe_2\{\eta,\eta\text{-}C_5H_4CH(NMePh)CH(NMePh)C_5H_4\}(CO)_2(\mu\text{-}CO)_2]$ (**2c**) (52% yield).

The yields of **1**–**3** depend on the volume of xylene used (Table 1) and on the molar ratio of reactants. With an excess of 6-dimethylaminofulvene (9 g, 75 mmol) over $[Fe(CO)_5]$ (9.8 g, 50 mmol) in xylene (70 cm^3), work-up as above gives **1** (53% yield) and **2** (27% yield), but no **3**.

2.2. *Preparation of R,S and R,R / S,S-$[Fe_2\{\eta,\eta\text{-}C_5H_4CH(NMe_2)CH(NMe_3)C_5H_4\}(CO)_2(\mu\text{-}CO)_2]X$, $[Fe_2\{\eta,\eta\text{-}C_5H_4CHC(NMe_3)C_5H_4\}(CO)_2(\mu\text{-}CO)_2][SO_3CF_3]$ and $[Fe_2\{\eta,\eta\text{-}C_5H_4CH_2CH(NMe_3)C_5H_4\}(CO)_2(\mu\text{-}CO)_2][SO_3CF_3]$ salts*

Solutions of **1** or **2** (1 g) were stirred with excess $MeOSO_2CF_3$ (1 cm^3) in benzene (70 cm^3) for 1 h or MeI (2 cm^3) in acetonitrile (20 cm^3) for 2 h. The products R,S or $R,R/S,S$-$[Fe_2\{\eta,\eta\text{-}C_5H_4CH(NMe_2)CH(NMe_3)C_5H_4\}(CO)_2(\mu\text{-}CO)_2]X$ ([**4**]X or [**5**]X respectively) ($X^- = I^-$ or SO_3CF_3-) separated either from the reaction mixtures (benzene solution) or on removal of the solvent (acetonitrile solution). They were filtered off, washed with benzene and pentane and recrystallized from dichloromethane–pentane mixtures if required (yields, *ca.* 75%).

Similarly, $MeOSO_2CF_3$ reacted slowly with the enamine $[Fe_2\{\eta,\eta\text{-}C_5H_4CHC(NMe_2)C_5H_4\}(CO)_2(\mu\text{-}CO)_2]$ (**6**) in benzene solution to given brown crystals of $[Fe_2\{\eta,\eta\text{-}C_5H_4CHC(NMe_3)C_5H_4\}(CO)_2(\mu\text{-}CO)_2][SO_3CF_3]$ ([**9**][SO_3CF_3]) with an 80% yield after

TABLE 1. Effects of reactant concentration on the yields of **1**–**3**

Xylene volume (cm^3)	Yield [a] (%)		
	1	2	3
30	0	8	83
50	11	15	59
70	46	12	38
100	62	14	20
150	75	20	0

[a] Of purified compounds from the reaction of $[Fe(CO)_5]$ (74.5 mmol) with 6-dimethylaminofulvene (50 mmol) in refluxing xylene after 2 h.

16 h, and with $[Fe_2\{\eta,\eta\text{-}C_5H_4CH_2CH(NMe_2)C_5H_4\}(CO)_2(\mu\text{-}CO)_2]$ (**7**) in chloroform solution to give red $[Fe_2\{\eta,\eta\text{-}C_5H_4CH_2CH(NMe_3)C_5H_4\}(CO)_2(\mu\text{-}CO)_2][SO_3CF_3]$, ([**10**]$[SO_3CF_3]$) with a 70% yield after 2 h.

2.3. Reactions of R,S-$[Fe_2\{\eta,\eta\text{-}C_5H_4CH(NMe_2)CH(NMe_3)C_5H_4\}(CO)_2(\mu\text{-}CO)_2]X$, R,R/S,S-$[Fe_2\{\eta,\eta\text{-}C_5H_4CH(NMe_2)CH(NMe_3)C_5H_4\}(CO)_2(\mu\text{-}CO)_2]X$ or $[Fe_2\{\eta,\eta\text{-}C_5H_4CH_2CH(NMe_3)C_5H_4\}(CO)_2(\mu\text{-}CO)_2][SO_3CF_3]$ with $[PhNMe_3]OH$

A mixture of *R,S*-$[Fe_2\{\eta,\eta\text{-}C_5H_4CH(NMe_2)CH(NMe_3)C_5H_4\}(CO)_2(\mu\text{-}CO)_2]X$ ([**4**]X) (2 g; $X^- = I^-$ or $SO_3CF_3{}^-$) in acetonitrile (100 cm^3) and an equimolar amount of a 40% solution of benzyltrimethylammonium hydroxide (Triton-B) in either methanol or water was stirred for 2–3 h. The solvent was then removed under reduced pressure, the residue extracted with dichloromethane (50 cm^3), and the extract washed twice with water; it was then dried over magnesium sulphate. Hexane was added to the solution, and the mixture cooled to −10°C to give the enamine $[Fe_2\{\eta,\eta\text{-}C_5H_4CHC(NMe_2)C_5H_4\}(CO)_2(\mu\text{-}CO)_2]$ (**6**) as red crystals. These were filtered off, washed with pentane and dried (yield, 50%).

Under the same conditions *R,R/S,S*-$[Fe_2\{\eta,\eta\text{-}C_5H_4CH(NMe_2)CH(NMe_3)C_5H_4\}(CO)_2(\mu\text{-}CO)_2]X$ ([**5**]X) gave the monoamine $[Fe_2\{\eta,\eta\text{-}C_5H_4CH_2CH(NMe_2)C_5H_4\}(CO)_2(\mu\text{-}CO)_2]$ (**7**) with about *ca.* 20% yield which is increased to 35% if CO gas is bubbled through the reaction mixture, and $[Fe_2\{\eta,\eta\text{-}C_5H_4CH_2CH(NMe_3)C_5H_4\}(CO)_2(\mu\text{-}CO)_2][SO_3CF_3]$, ([**10**]$[SO_3CF_3]$) gave $[Fe_2\{\eta,\eta\text{-}C_5H_4CH_2CH_2C_5H_4\}(CO)_2(\mu\text{-}CO)_2]$ (**11**) with a 20% yield.

2.4. Reactions of R,S-$[Fe_2\{\eta,\eta\text{-}C_5H_4CH(NMe_2)CH(NMe_3)C_5H_4\}(CO)_2(\mu\text{-}CO)_2]X$, R,R/S,S-$[Fe_2\{\eta,\eta\text{-}C_5H_4CH(NMe_2)CH(NMe_3)C_5H_4\}(CO)_2(\mu\text{-}CO)_2]X$, $[Fe_2\{\eta,\eta\text{-}C_5H_4CHC(NMe_3)C_5H_4\}(CO)_2(\mu\text{-}CO)_2][SO_3CF_3]$ and $[Fe_2\{\eta,\eta\text{-}C_5H_4CH_2CH(NMe_3)C_5H_4\}(CO)_2(\mu\text{-}CO)_2][SO_3CF_3]$ with $LiAlH_4$

Fresh $LiAlH_4$ (0.2 g) was added to a solution of *R,S*-$[Fe_2\{\eta,\eta\text{-}C_5H_4CH(NMe_2)CH(NMe_3)C_5H_4\}(CO)_2(\mu\text{-}CO)_2]X$ ([**4**]X) or *R,R/S,S*-$[Fe_2\{\eta,\eta\text{-}C_5H_4CH(NMe_2)CH(NMe_3)C_5H_4\}(CO)_2(\mu\text{-}CO)_2]X$ ([**5**]X) (1 g) ($X^- = I^-$ or $SO_3CF_3{}^-$) in tetrahydrofuran (50 cm^3) which had been dried over sodium–benzophenone. A rapid reaction took place, and trimethylamine was evolved. The mixture was stirred for 3 h. The solvent was then removed at reduced pressure, and the residue recrystallized from a dichloromethane–hexane mixture to give $[Fe_2\{\eta,\eta\text{-}C_5H_4CH_2CH(NMe_2)C_5H_4\}(CO)_2(\mu\text{-}CO)_2]$ (**7**) as a bright-red powder (yield, 85%).

$LiAlD_4$ gave $[Fe_2\{\eta,\eta\text{-}C_5H_4CHDCH(NMe_2)C_5H_4\}(CO)_2(\mu\text{-}CO)_2]$ (**7-D**).

Under the same conditions, $LiAlH_4$ reduced $[Fe_2\{\eta,\eta\text{-}C_5H_4CH_2CH(NMe_3)C_5H_4\}(CO)_2(\mu\text{-}CO)_2][SO_3CF_3]$ ([**10**]$[SO_3CF_3]$) to red $[Fe_2\{\eta,\eta\text{-}C_5H_4CH_2CH_2C_5H_4\}(CO)_2(\mu\text{-}CO)_2]$ (**11**) (yield, 70%) and $[Fe_2\{\eta,\eta\text{-}C_5H_4CHC(NMe_3)C_5H_4\}(CO)_2(\mu\text{-}CO)_2][SO_3CF_3]$ ([**9**]$[SO_3CF_3]$) to an inseparable mixture of $[Fe_2\{\eta,\eta\text{-}C_5H_4CH_2CH_2C_5H_4\}(CO)_2(\mu\text{-}CO)_2]$ (**11**) and $[Fe_2\{\eta,\eta\text{-}C_5H_4CHCHC_5H_4\}(CO)_2(\mu\text{-}CO)_2]$ (**12**), (ratio, 3:1; yield, 70%).

2.5. Acid-catalysed hydrolysis of $[Fe_2\{\eta,\eta\text{-}C_5H_4CHC(NMe_2)C_5H_4\}(CO)_2(\mu\text{-}CO)_2]$

A solution of concentrated hydrochloric acid (0.5 cm^3) in water (5 cm^3) was added to one of $[Fe_2\{\eta,\eta\text{-}C_5H_4CHC(NMe_2)C_5H_4\}(CO)_2(\mu\text{-}CO)_2]$ (**6**) (1 g) in acetonitrile (50 cm^3), and the mixture was stirred for 2 h. The solvent was then removed under reduced pressure, the residue extracted with dichloromethane (50 cm^3), and the extract washed twice with water; it was then dried over magnesium sulphate. Hexane was added, and the solution kept at −10°C overnight to give purple crystals of the ketone $[Fe_2\{\eta,\eta\text{-}C_5H_4CH_2C(O)C_5H_4\}(CO)_2(\mu\text{-}CO)_2]$ (**8**). These were filtered off, washed with pentane and dried (yield, 70%).

2.6. Reactions of $[Fe_2\{\eta,\eta\text{-}C_5H_4CH_2C(O)C_5H_4\}(CO)_2(\mu\text{-}CO)_2]$ with $2,4\text{-}(NO_2)_2\text{-}C_6H_3NHNH_2 \cdot H_2SO_4$, $NH_2CONHNH_2 \cdot HCl$, $NH_2NH_2 \cdot H_2O$ and $NH_2OH \cdot HCl$

These were carried out as described in ref. 6, with minor variations, to give the following compounds after recrystallization from dichloromethane–pentane mixtures: orange $[Fe_2\{\eta,\eta\text{-}C_5H_4CH_2C(NNHC_6H_3(NO_2)_2\text{-}2,4)C_5H_4\}(CO)_2(\mu\text{-}CO)_2]$ (**13**) (yield, 50%); purple $[Fe_2\{\eta,\eta\text{-}C_5H_4CH_2C(NNHCONH_2)C_5H_4\}(CO)_2(\mu\text{-}CO)_2]$ (**14**) (yield, 60%); purple $[Fe_2\{\eta,\eta\text{-}C_5H_4CH_2C(NNH_2)C_5H_4\}(CO)_2(\mu\text{-}CO)_2]$ (**15**) (yield, 65%); red-brown $[Fe_2\{\eta,\eta\text{-}C_5H_4CH_2C(NOH)C_5H_4\}(CO)_2(\mu\text{-}CO)_2]$ (**16**) (yield, 75%).

2.7. Reduction of $[Fe_2\{\eta,\eta\text{-}C_5H_4CH_2C(O)C_5H_4\}(CO)_2(\mu\text{-}CO)_2$ with $LiAlH_4$

A 10:1 molar excess of $LiAlH_4$ was added to a solution of $[Fe_2\{\eta,\eta\text{-}C_5H_4CH_2C(O)C_5H_4\}(CO)_2(\mu\text{-}CO)_2]$ (**8**) (0.5 g) in diethylether (70 cm^3). After 5 min the mixture was hydrolysed by the dropwise addition of water (40 cm^3) containing NaOH (0.52 g). The ethereal layer was separated and washed with water, and the solvent removed under reduced pressure. The residue was extracted with dichloromethane and the extract dried over magnesium sulphate. Partial removal of the solvent, addition of hexane, and cooling to −10°C gave red crystals of $[Fe_2\{\eta,\eta\text{-}C_5H_4CH_2CH(OH)C_5H_4\}$-

TABLE 2. Melting points and analyses for the compounds described in the text

Compound [a]	Melting point [b] (°C)	Analysis [c]			
		(%) C	(%) H	(%) N	(%) Fe
1	175–177	51.9 (51.4)	4.7 (4.7)	6.0 (6.0)	23.6 (23.9)
2	237–240	51.6 (51.4)	4.7 (4.7)	6.0 (6.0)	23.7 (23.9)
2a	188–189	54.7 (55.2)	6.2 (5.8)	5.2 (5.4)	
2b	209–210	60.3 (60.5)	6.4 (6.7)	4.2 (4.5)	17.2 (17.9)
[d]	112–113	57.6 (57.9)	6.7 (6.9)	4.5 (4.8)	19.5 (19.3)
2c · $\frac{1}{2}C_7H_8$	161–163	57.6 (57.8)	4.1 (4.6)	4.1 (4.4)	17.4 (17.7)
3	200	50.6 (50.8)	3.4 (3.3)	3.1 (3.1)	
3a	129–130	53.0 (52.8)	4.2 (4.0)	2.9 (2.9)	
3b	202–203	55.0 (54.8)	4.5 (4.4)	2.7 (2.9)	21.6 (22.2)
6	260 dec.	51.0 (51.4)	3.7 (3.6)	3.3 (3.3)	26.5 (26.5)
7	245 dec.	51.2 (51.1)	4.1 (4.0)	2.9 (3.3)	26.1 (26.5)
8	213–215	48.5 (48.8)	2.5 (2.6)		27.9 (28.4)
[**9**][CF_3SO_3]	198–200	40.8 (41.1)	2.9 (3.1)	2.2 (2.4)	18.6 (18.9)
[**10**][CF_3SO_3]	202 dec.	39.4 (39.7)	3.3 (3.8)	2.3 (2.3)	18.3 (18.5)
11	209 dec	50.9 (50.5)	3.1 (3.4)		
13	240–242	45.7 (46.0)	2.5 (2.5)	9.9 (9.8)	19.0 (19.5)
14 · H_2O	222–225	43.4 (43.5)	3.3 (3.2)	8.5 (9.0)	23.4 (23.8)
15	248–252	46.8 (47.1)	2.6 (2.7)	6.8 (6.9)	26.9 (27.4)
16 · CH_2Cl_2	237–239	41.0 (41.3)	2.6 (2.7)	2.8 (2.8)	22.7 (22.6)
17 · CH_2Cl_2	188–191	48.3 (48.5)	2.8 (3.1)		28.0 (28.2)

[a] See text.

[b] Determined in sealed tubes; dec., decomposition.

[c] Found (calculated).

[d] $[Fe_2(C_5H_4CH_2N^iPr_2)_2(CO)_4]$.

TABLE 3. IR spectra (1650–2050 cm^{-1} region) of the compounds described in the text

Compound	Absorption bands [a] (cm^{-1})				
1 [b]	1792 (8.4)	1811 (sh)	1965 (1.8)	2003 (10)	
2 [b]	1791 (6.4)	1808 (sh)	1967 (1.8)	2004 (10)	
2a [b]	1791 (12.8)	1811 (sh)	1966 (3.4)	2004 (10)	
2b [b]	1789 (8.8)	1811 (0.2)	1966 (2.7)	2000 (10)	
[c]	1782 (11.7)	1810 (0.1)	1956 (13.5)	2000 (10)	
2c [d]	1767 (9.0)	1800 (sh)	1965 (6.5)	1991 (10)	
3 [b]	1930 (1.9)	1962 (6.0)	1984 (9.9)	2032 (10)	ν(C=N) 1614(2.0) [e]
3a [b]	1935 (1.8)	1962 (5.9)	1980 (10)	2032 (8.5)	ν(C=N) 1620(2.5) [e]
3b [b]	1934 (2.1)	1963 (6.3)	1979 (10)	2031 (8.8)	ν(C=N) 1607(3.7) [e]
6 [d]	1775 (5.2)	1812 (sh)	1961 (2.0)	2001 (10)	ν(C=C) 1625 (w)
7 [d]	1768 (4.5)		1960 (1.7)	2002 (10)	
8 [d]	1781 (5.3)	1817 (0.7)	1971 (1.6)	2011 (10)	ν(CO) 1687 (w)
[**9**]$^+$ [d,f]	1790 (6.6)	1821 (1.1)	1973 (1.9)	2012 (10)	ν(C=C) 1654 (w)
[**10**]$^+$ [d,f]	1780 (5.0)	1810 (0.6)	1975 (1.5)	2013 (10)	
11 [d]	1767 (5.7)		1958 (2.3)	2001 (10)	
13 [g]	1781 (5.0)	1805 (0.5)	1960 (2.0)	1998 (10)	
14 [d]	1775 (5.3)	1814 (sh)	1968 (1.8)	2007 (10)	
15 [d]	1772 (5.2)	1809 (sh)	1963 (1.6)	2003 (10)	ν(C=N) 1625 (w), ν(NH) 3413
16 [d]	1773 (5.2)	1805 (sh)	1964 (1.6)	2005 (10)	ν(C=N) 1629 (w)
17 [d]	1769 (5.0)	1807 (sh)	1959 (2.0)	2002 (10)	

[a] Peak positions with relative peak heights in parentheses: sh, shoulder; w, weak. Absorption bands due to ν(CO) vibrations unless it is stated otherwise.

[b] Spectra run in hexane solution.

[c] $[Fe_2\{\eta^5\text{-}C_5H_4CH_2N^iPr_2\}_2(CO)_2(\mu\text{-}CO)_2]$.

[d] Spectra run in chloroform solution.

[e] Due to ν(CN) vibration of exocyclic C–N.

[f] As $[CF_3SO_3]^-$ salts.

[g] Spectrum run in carbon disulfide solution.

TABLE 4. ^1H NMR spectra of the $[Fe_2\{\eta^5,\eta^5\text{-}C_5H_4CH(NR_2)CH(NR_2)C_5H_4\}(CO)_2(\mu\text{-}CO)_2]$ complexes **1**, **2**, **2a–2c** and $[Fe_2\{\eta^5\text{-}C_5H_4CH_2N^iPr_2\}_2(CO)_2(\mu\text{-}CO)_2]$ at various temperatures.

A–B	T (K)	Resonances [a], δ (ppm)		
		η-C_5H_4 [b]	CH	NR_2
R,S-CH(NMe_2)CH(NMe_2) (**1**)	298	5.23 (2), 5.06 (2), 5.00 (2), 4.85 (2)	3.01 (2)	2.21 (12)
	178	5.38 (1), 5.25 (1), 5.15 (1), 5.13 (1)	3.05 (1)	2.39 (3) 2.00 (6) 1.97 (3)
		5.04 (1), 5.01 (1), 4.95 (1), 4.87 (1)	2.81 (1)	
$R,R/S,S$-CH(NMe_2)CH(NMe_2) (**2**)	298	5.20 (2), 5.11 (2), 4.68 (2), 4.59 (2)	2.81 (2)	1.91 (12)
	178	5.31 (2), 5.23 (2), 4.79 (2), 4.69 (2)	2.86(2)	2.01(6) 1.72(6)
$R,R/S,S$-CH(NEt_2)CH(NEt_2) (**2a**)	298	5.22 (2) 5.08 (2) 4.70 (2) 4.62 (2)	3.09(2)	2.34 (4,sx), 1.76 (4,sx)
				0.98 (12, t, J = 7.0 Hz) [c]
	193	5.31 (2), 5.15 (2), 4.73 (2), 4.69 (2)	3.07 (2)	2.43 (2,sx), 1.93 (2,sx), 1.03(6,t J = 6.4 Hz) [d]
				2.17 (2,sx), 1.36 (2,sx), 0.91 (6,t,J = 6.6 Hz) [e]
$R,R/S,S$-CH(N^iPr_2)CH(N^iPr_2) (**2b**) [f]	373	4.84 (2), 4.73 (4), 4.59 (2)	3.39 (2)	2.77 (4,sp, J = 6.8 Hz), 1.11 (12,d), 0.76 (12,br)
	253	4.65 (2), 4.59 (2), 4.56 (2), 4.35 (2)	3.21 (2)	2.59 (2,sp, J = 6.8 Hz) 2.46 (2,sp,J = 6.8)
				1.17 (6,d) 0.94 (6,d) 0.94 (6,d) 0.31 (6,d)
[g]	293	4.56 (4), 4.38 (4)	3.48 (4)	3.00 (4,sp,J = 6.8) 1.15 (24,d)
	193	4.58 (br), 4.55 (br), 4.46 (br)	3.51	2.97 (4,br,m), 1.01 (24,br,m)
		4.40 (br)	3.40	
$R,R/S,S$-CH(NMePh)CH(NMePh) (**2c**)	298	5.23 (4), 5.17 (2), 4.93 (2)	4.79 (2)	6.5–7.1 (10,m) [h], 2.7 (6)
	177	5.2–4.8 [i]	4.41 (1)	6.4–7.2 (10,m) [h], 3.25 (3) 2.24 (3)
			3.25 (1)	

[a] Downfield from Me_4Si as an internal standard in CS_2–CD_2Cl_2 solution (4 : 1). All resonances are singlets unless it is stated otherwise. Relative integrations in parentheses together with the following: d, doublet; t, triplet, q, quartet, p, quintet; sx, sextet; sp, septet; m, multiplet; br, broad; coupling constants J. Solvent resonances at 5.32 δ may partially obscure some resonances.

[b] All C_5H_4 resonances are multiplets.

[c] J_{AB} = 13 Hz.

[d] J_{AB} = 13.1 Hz.

[e] J_{AB} = 12.1 Hz.

[f] $C_6D_5CD_3$ solution.

[g] Unlinked dimer $[Fe_2(\eta^5\text{-}C_5H_4CH_2N^iPr_2)_2(CO)_4]$; *cis* : *trans* ratio = 65 : 35 at 193 K.

[h] Resonances due to Ph protons.

[i] Four broad and ill-resolved resonances. Low temperature limit not reached.

$(CO)_2(\mu\text{-}CO)_2]$ (**17**) which were filtered off, washed with pentane and dried (yield, 70%).

The melting points and analyses of the various products are summarized in Table 2; their IR bands between 1600 and 2100 cm^{-1} are shown in Table 3, their ^1H NMR data in Tables 4–6, and some ^{13}C NMR data in Table 7.

2.8. X-Ray crystallography

2.8.1. Structure of R,R / S,S-$[Fe_2\{\eta,\eta\text{-}C_5H_4CH(NMe_2)CH(NMe_2)C_5H_4\}(CO)_2(\mu\text{-}CO)_2]$ (2); crystal data

$C_{20}H_{22}N_2O_4Fe_2$; M_r = 466.0; tetragonal; space group, $I\bar{4}2d$ (No. 122); a = 18.022(9) Å and c = 12.654(5) Å; U = 4110.0 Å^3; Z = 8; D_m (by flotation) = 1.50 Mg cm^{-3} and D_c = 1.506 Mg cm^{-3}; $F(000)$ = 1920; μ(Mo Kα) = 14.4 cm^{-1}. Unit-cell parameters initially were obtained from precession photographs using Mo Kα radiation and, more accurately, by a least-squares fit to diffractometer data. The crystal for the data collection was 0.4 mm × 0.2 mm × 0.2 mm in size. Intensities were collected at −100°C on a Nicolet XRD P3 four-circle diffractomer in the range 4.0° > 2θ > 55.0° using monochromated Mo Kα radiation. Reflections were corrected for Lorentz, polarization and absorption effects; for the latter the empirical corrections gave transmission factors of 0.815 and 0.683 respectively. 2633 reflections were measured, and yielded 1375 unique reflections, Friedel opposites merged, of which 947 had $I > 3\sigma(I)$ and were used for the structure analysis. The structure was solved by the heavy-atom method. Difference maps were used to locate the approximate positions of the hydrogen atoms and these positions were optimized assuming C–H to be 1.0 Å. The structure was refined by the full-matrix least-squares method in which the function minimized was $\Sigma w\Delta^2$ where $w = 1/\sigma(F)$. Hydrogen atom parameters were not refined. The anisotropic refinement was terminated when the maximum parameter shift was less than 0.1σ. Final values for R and R_w $(=(\Sigma w\Delta^2/\Sigma w|F_o|^2)^{1/2})$ were 0.032 and 0.020 respectively. A final difference map showed no unusual features, with a maximum residual electron density of $<|0.4|$ e Å^{-3}. All calculations were carried out on a IBM 486 computer using programs written by F.S. Stephens. Neutral

TABLE 5. ^1H NMR spectra of some of the $[Fe_2\{\eta,\eta\text{-}C_5H_4\text{-A-B-}C_5H_4\}(CO)_2(\mu\text{-}CO)_2]$ derivatives described in the text

A-B	Resonances [a], δ (ppm)		
	C_5H_4 [b]	C-H	NMe_2 or NMe_3
R,S-$CH(NMe_2)CH(NMe_3^+)$, [**4**][SO_3CF_3]	5.46 (1), 5.39 (3), 5.35 (1) 5.28 (2), 5.14 (1)	4.49 (2)	NMe_3 3.18 (9), NMe_2 2.90 (3), 2.59 (3)
R,R/S,S-$CH(NMe_2)CH(NMe_3^+)$, [**5**][SO_3CF_3] [c]	5.55 (3), 5.45 (1), 5.36 (1) 5.27 (1), 4.99 (1), 4.90 (1)	4.30 (d,1), 3.56 (d,1) (*J* = 11.7 Hz)	NMe_3 2.89 (9), NMe_2 2.43 (3) 1.69 (3)
$CHC(NMe_2)$ (**6**)	5.32 (2), 5.25 (2), 4.64 (2), 4.43 (2)	4.67 (1)	2.49 (6)
$CH_2CH(NMe_2)$ (**7**)	5.35 (1), 5.23 (3), 4.93 (1), 4.85 (2), 4.72 (1)	H_A 3.04 (1), H_B 2.36 (1), H_C 2.03 (1) [d]	2.03 (6)
$CH(D)CH(NMe_2)$ (**7-D**)	5.34 (1), 5.23 (3), 4.93 (1), 4.85 (2), 4.72 (1)	H_A 3.03 (1), H_C 1.98 (1) [e]	2.03 (6)
$CH_2C(O)$ (**8**)	5.45 (4,s), 5.30 (2), 5.00 (2)	2.95 (2)	
$CHC(NMe_3^+)$, [**9**][SO_3CF_3] [c]	5.62 (2), 5.52 (2), 5.23 (2), 4.90 (2)	3.39 (1)	3.08 (9)
$CH_2CH(NMe_3^+)$, [**10**][SO_3CF_3] [c]	5.62, (1), 5.53 (1), 5.48 (1), 5.36 (3), 5.04 (2)	H_A 3.90 (1), H_B 2.81 (1), H_C 2.32 (1) [f]	2.82 (9)
CH_2CH_2 (**11**)	5.21 (4), 4.83 (4)	2.16 (4)	
CHCH (**12**)	5.31 (4), 4.51 (4)	6.23 (2)	
$CH_2C(NNH_2)$ (**15**)	5.35 (2), 5.25 (2), 5.20 (2), 4.79 (2)	2.76 (2)	NH_2 5.44 (2)

[a] Downfield from Me_4Si as an internal standard in $CDCl_3$ solution. All resonances are singlets unless it is stated otherwise. Relative integrations in parentheses together with the following: s, singlet; m, multiplet; br, broad, coupling constants *J*. All spectra run at 293 K.

[b] All C_5H_4 resonances are multiplets unless it is stated otherwise.[c] CD_3CN solution.

[d] $J_{AB} = 2.4$ Hz, $J_{AC} = 12.6$ Hz and $J_{BC} = 14.8$ Hz.

[e] $J_{AC} = 12.6$ Hz.

[f] $J_{AB} = 2.2$ Hz, $J_{AC} = 12.6$ Hz and $J_{BC} = 14.8$ Hz.

TABLE 6. ^{1}H NMR spectra of [$Fe_2(\eta^3,\eta^5\text{-}R_2NCHC_5H_3CHC_5H_4)(CO)_5$], **3**, **3a** and **3b**, in CS_2–CD_2Cl_2 solution (4:1)

R	*T* (K)	Resonances [a,b], δ (ppm)						
		R_2N	H(8)	H(1)–H(4)	H(9)	H(6)	H(10)	H(12)
Me (**3**)	294	3.24	2.78	3.86, 3.92, 4.70, 4.75	6.04 (br)	6.13	6.84 (d, J = 4.9 Hz)	7.33
	183	3.38 3.76	2.78	3.75, 3.96, 4.78, 4.80	5.98 (br)	6.15	6.89 (d, J = 4.9 Hz)	7.43
Et (**3a**)	291	1.31 (t, J = 6.9 Hz), 3.49 (dect)	2.81	3.91, 3.96, 4.73, 4.78	6.05 (br)	6.17	6.79 (d, J = 4.8 Hz)	7.39
	183	1.24 (t, J = 6.8 Hz), 1.35 (t, J = 6.9 Hz), 3.46 (m,br)	2.80	3.81, 3.91, 4.81, 4.81	6.01 (br)	6.18	6.81 (d, J = 4.8 Hz)	7.39
^{i}Pr (**3b**)	294	1.37 (d, J = 6.8 Hz), 1,35 (d, J = 7.3 Hz), 4.15 (m,br)	2.92	4.04, 4.14, 4.77, 4.85	6.17 (br)	6.23	6.88 (d, J = 5.5 Hz)	7.60
	223	1.26 (br,3), 1.39 (d, J = 6.6 Hz, 6), 1.50 (br,3) 3.76 (br,1), 4.51 (br,1)	2.92	3.96, 4.11, 4.84, 4.91	6.19 (br)	6.29	6.95 (d, J = 5.0 Hz)	7.63

[a] Downfield from Me_4Si as an internal standard. Singlets unless it is stated otherwise; d, doublet; dect, dectet; m, multiplet; br, broad. Coupling constants *J*. All resonances integrate as required by the formulae except for **3b** where intensities of the ^{i}Pr protons are included in the parentheses.

[b] For assignment see text.

atom scattering factors were taken from ref. 7, with corrections for anomalous dispersion. A perspective drawing of the molecule [8], together with the atom labelling scheme, is shown in Fig. 2. The non-hydrogen atomic coordinates are listed in Table 9, and bond lengths and angles in Table 10; in Table 11, selected bond lengths and angles are compared with those previously reported for **1** [2]. Tables of anisotropic thermal parameters, hydrogen atom parameters, intermolecular contacts and mean planes data have been deposited with the Cambridge Crystallographic Data Centre.

2.8.2. Structure of [$Fe_2\{\eta,\eta\text{-}C_5H_4CH_2C(O)C_5H_4\}(CO)_2(\mu\text{-}CO)_2$] (8); Crystal data

$C_{16}H_{10}O_5Fe_2$; M_r = 393.9; monoclinic; space group, $P2_1/n$; a = 7.263(2) Å, b = 22.296(4) Å and c = 8.982(2) Å; β = 96.62(2)°; U = 1444.8 Å^3; Z = 4; $F(000)$ = 791.93; μ(Mo Kα) = 19.34 cm^{-1}. The crystal used for the data collection, 0.24 mm × 0.27 mm × 0.28 mm in size, was cut from a larger crystal grown from dichloromethane solution. Unit-cell dimensions were determined from diffractometer data. Intensities were collected on an Enraf–Nonius CAD4 diffractometer using the ω–2θ scan method in the range $2° < 2\theta < 48°$ with μ(Mo Kα) radiation (λ = 0.7093 Å) and a graphite monochromator. Data were corrected for Lorentz and polarization effects but not for absorption.

The structure was solved by Patterson methods, SHELX86 [9], and refined by the full-matrix least-squares method, SHELX76 [10], using 3284 unique reflections of which 2250 had $I > 3\sigma I$, and 248 variable parameters. Hydrogen atoms were refined isotropically and all other atoms were refined anisotropically. The refinement was terminated when the maximum parameter shift was less than 0.001σ. Final values for $R = [\Sigma | F_o - F_c | / \Sigma | F_o |]$ and $R_w = \{[\Sigma w(| F_o - F_c |)^2]/[\Sigma(| F_o |)^2]\}^{1/2}$ where $w = 1/[(\sigma F_o)^2 - 0.0027F_o^2]$ are 0.0254 and 0.0247 respectively. A final difference Fourier map showed residual peaks with a maximum of 0.23 e Å^{-3} and a minimum of −0.14 e Å^{-3}. All calculations were carried out on a VAX 8700 computer. The atomic scattering factors for non-hydrogen and hydrogen atoms, and the anomalous dispersion correction factors for non-hydrogen atoms were taken from the literature [11–13]. A perspective drawing of the molecule [8] with the atom labelling scheme is given in Fig. 3. The atom coordinates are given in Table 12, and bond lengths and bond angles in Table 13. Tables of thermal parameters and hydrogen atom thermal parameters have been deposited at the Cambridge Crystallographic Data Centre.

3. Results and discussion

The reactions investigated during this work are outlined in Scheme 1, and the complexes prepared are listed in Table 2 together with their melting points and analyses. All are brown to purple solids soluble in the anticipated organic solvents and reasonably stable in the solid state, but most are oxidized slowly in solution.

6-Dimethylaminofulvene reacts with [$Fe(CO)_5$] in refluxing xylene to give three products **1–3**, with evolution of CO and an unidentified volatile amine. The brown–purple **1** and the red **2** are isomers of [$Fe_2\{\eta,\eta\text{-}C_5H_4CH(NMe_2)CH(NMe_2)C_5H_4\}(CO)_2(\mu\text{-}CO)_2$] whilst the brown **3** is [$Fe_2\{\eta^3,\eta^5\text{-}Me_2NCHC_5H_3\text{-}CHC_5H_4\}(CO)_5$]. *

The yields of **1–3** are a function of the reagent concentrations (Table 1) and ratios. With an excess of [$Fe(CO)_5$], the yields of **1** and **2** increase as the reaction volume is increased (from 0 to 75% and from 8 to

---

* The structure of **3** was determined by an X-ray diffraction study [14] and shown to be identical with that reported previously [3].

TABLE 7. ^{13}C NMR spectra at 295 K of some of the compounds described in the text

R_2N or A–B	Resonances [a], δ (ppm)				
	R_2N	CH	C_5H_4	CO	μ-CO
[$Fe_2\{\eta,\eta\text{-}C_5H_4CH(NR_2)CH(NR_2)C_5H_4\}(CO)_2(\mu\text{-}CO)_2$] derivatives					
Me_2N (**1**)	45.2	65.4	79.5, 84.6, 94.2, 95.0, 100.8	210.3	273.7, 273.9
Me_2N (**2**)	40.5	60.7	80.6, 83.2, 92.3, 93.1, 96.3	210.0	272.7
Et_2N (**2a**)	13.5, 42.9	54.9	80.6, 83.3, 91.6, 95.7, 95.2	210.1	273
$^iPr_2N$ (**2b**)	17.8, 23.0, 24.8, 26.2, 46.8, 46.9	54.7	80.3, 83.7, 91.4, 94.8, 99.9	210.9	270.6
PhMeN (**2c**)	36.4, 113.7, 118.4, 129.3, 149.1	59.3	82.1, 82.3, 93.9, 96.2, 98.8	209.5	272.2
	A–B		C_5H_4	CO	μ-CO
[$Fe_2\{\eta,\eta\text{-}C_5H_4\text{–}A\text{–}B\text{–}C_5H_4\}(CO)_2(\mu\text{-}CO)_2$] derivatives					
$CH_2CH(NMe_2)$ (**7**)	CH_2 29.1, CH 60.7, NMe_2 40.9		80.7, 81.6, 82.6, 84.1, 91.7, 92.4, 94.0, 96.3, 96.9, 98.7	209.57, 209.62	272.3, 272.6
$CH_2C(O)$ (**8**)	CH_2 37.9, C(O) 194.2		83.2, 85.9, 89.1, 94.2, 94.3, 96.4	209.1(br)	267.8(br)
$CH_2CH(NMe_3^+)$ ([**10**][SO_3CF_3]) [b]	CH_2 25.8, CH 71.0, NMe_3 52.5		83.1, 84.2, 85.5, 86.1, 90.7, 93.0, 94.2, 97.1, 97.6, 99.5		
CH_2CH_2 (**11**)	CH_2 23.9		82.0, 93.9, 99.8	209.8	273.0
CHCH (**12**)	CH 125.9		84.0, 91.9, 95.5	209.8	272.9
	R_2N		Organic ligand		CO
[$Fe_2(\eta^3,\eta^5\text{-}R_2NCHC_5H_3CHC_5H_4)(CO)_5$] derivatives					
Me_2N (**3**)	43.5		38.0, 71.4, 80.1, 83.5, 85.2, 110.1, 112.3, 124.3, 128.4, 138.1		215.3, 218.1, 219.9
Et_2N (**3a**)	13.7, 43.3		37.7 [c], 71.2, 71.7, 79.7, 83.2, 83.4, 84.9, 107.8, 109.7, 111.7, 112.6, 123 [c], 127 [c], 135.7, 137.5		214.4, 217.2 [b], 219.0 [b]
$^iPr_2N$ (**3b**)	21.9(br), 48.9(br)		37.4, 71.4, 71.7, 80.1, 83.7, 84.0, 85.0, 108.4, 113.4, 124.4, 128.2, 132.6		215.6, 218.2, 220.0

[a] Downfield from Me_4Si as an internal standard in $CDCl_3$ solution unless it is otherwise stated. All resonances are singlets: br, broad. For assignment see text.

[b] CD_3CN solution.

[c] These resonances have more than one component. See text.

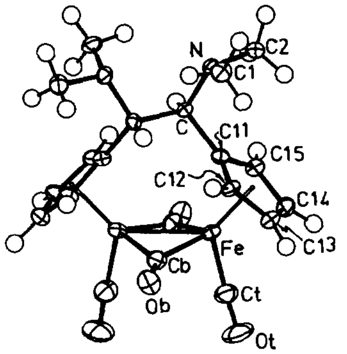

Fig. 2. The molecular structure and atom-labelling scheme for S,S-$[Fe_2\{\eta^5,\eta^5-C_5H_4CH(NMe_2)CH(NMe_2)C_5H_4\}(CO)_2(\mu-CO)_2]$ (**2**).

20% respectively), but that of **3** decreases from 83 to 0% (*cf.* ref. 1). With an excess of $[C_5H_4CHNMe_2]$, no **3** is obtained.

Similar reactions between $[Fe(CO)_5]$ and other 6-aminofulvenes give analogues of **2** and **3** but not **1**: $[Fe_2\{\eta,\eta-C_5H_4CH(NEt_2)CH(NEt_2)C_5H_4\}(CO)_2(\mu-CO)_2]$ (**2a**); $[Fe_2\{\eta,\eta-C_5H_4CH(N^iPr_2)CH(N^iPr_2)C_5H_4\}(CO)_2(\mu-CO)_2]$ (**2b**); $[Fe_2\{\eta,\eta-C_5H_4CH(NMePh)CH(NMePh)C_5H_4\}(CO)_2(\mu-CO)_2]$ (**2c**); $[Fe_2\{\eta^3,\eta^5-Et_2NCHC_5H_3CHC_5H_4\}(CO)_5]$ (**3a**); $[Fe_2\{\eta^3,\eta^5-{}^iPr_2NCHC_5H_3CHC_5H_4\}(CO)_5]$, (**3b**) traces of $[Fe_2\{\eta^3,\eta^5-MePhNCHC_5H_3CHC_5H_4\}(CO)_5]$. 6-di-isopropylaminofulvene also gives the unlinked complex $[Fe_2(\eta^5-C_5H_4CH_2N^iPr_2)_2(CO)_4]$.

The reaction of the fulvenes with $[Fe(CO)_5]$ probably proceeds via $[Fe(\eta^4\text{-fulvene})(CO)_n]$ intermediates ($n = 2$ or 3) (*cf.* ref. 15), which dimerize to **1** or **2**. The absence of counterparts of **1** with the more bulky R_2N may be due to steric factors that affect the formation of the linking C–C bond and, in the case of the very bulky $^iPr_2N$ group, allow hydrogen abstraction from the solvent to be competitive. The source of **3** is not clear. The data in Table 1 imply that **3** is derived from **1** provided that an excess of $[Fe(CO)_5]$ is present in the

TABLE 8. Coalescence temperatures T_c and activation energies ΔG_{T_c} for fluxional processes discussed in the text

Compound	Resonance	T_c (K)	ΔG_{T_c} (kcal mol^{-1})
1	CHCH [a]	220	10.6
1	C_5H_4 [a]	219	10.6
1	C_5H_4 [a]	213	10.6
1	Me_2N [b]	191	8.9
1	μ-CO [c]	378	15.6
2	Me_2N	191	8.9
2a	Et_2N [b]	220	10.9
2b	$^iPr_2N$ [b]	333, 318, 313	15.6
2c	MeN [b]	196	8.8
2c	CHCH [b]	188	8.4
2c	Ph [b]	182	8.8
3	Me_2N [d]	213	10.4
3a	Et_2N [d]	225	10.9
3b	$^iPr_2N$ [d]	253, 268	13.5

[a] Partial rotation about ring-linking C–C bond.
[b] Rotation-inversion of R_2N group.
[c] μ-CO–μ-CO site exchange.
[d] Rotation about C–NR_2 bond.

TABLE 9. Final atomic parameters (coordinates × 10^4) for the non-hydrogen atoms with estimated standard deviations in parentheses of $R,R/S,S$-$[Fe_2\{\eta,\eta-C_5H_4CH(NMe_2)CH(NMe_2)C_5H_4\}(CO)_2(\mu-CO)_2]$ (**2**)

Atom	x	y	z	B_{eq}
Fe	3182.8(5)	1790.5(4)	3919.8(6)	2.2
C(b)	2376(3)	1629(3)	4849(4)	2.9
O(b)	2253(2)	1521(2)	5762(3)	3.9
C(t)	3380(4)	837(3)	3969(5)	4.1
O(t)	3523(2)	218(2)	3963(4)	6.7
C(11)	3365(3)	2953(2)	3810(4)	2.1
C(12)	3503(3)	2710(3)	4861(4)	2.3
C(13)	4064(3)	2185(3)	4835(4)	2.6
C(14)	4291(3)	2100(3)	3751(6)	3.7
C(15)	3864(3)	2575(3)	3137(4)	2.5
C	2876(3)	3606(2)	3456(4)	2.0
N	3275(2)	4316(2)	3611(3)	2.5
C(1)	3431(3)	4510(3)	4721(4)	3.3
C(2)	3945(3)	4369(3)	2961(4)	3.1

TABLE 10. Selected molecular dimensions with estimated standard deviations in parentheses of $R,R/S,S$-$[Fe_2\{\eta,\eta-C_5H_4CH(NMe_2)CH(NMe_2)C_5H_4\}(CO)_2(\mu-CO)_2]$ (**2**) [a]

(a) Distances (Å)			
Fe–Fe′	2.498(2)		
Fe–C(b)	1.891(6)	Fe–C(b′)	1.917(5)
Fe–C(t)	1.756(5)	Fe–Cp	1.734
C(b)–O(b)	1.193(5)	C(t)–O(t)	1.146(6)
C(11)–C(12)	1.423(6)	C(11)–C	1.536(5)
C(12)–C(13)	1.385(6)	C–C′	1.546(9)
C(13)–C(14)	1.440(8)	C–N	1.482(5)
C(14)–C(15)	1.389(7)	N–C(1)	1.475(5)
C(15)–C(11)	1.414(6)	N–C(2)	1.464(6)
(b) Angles (°)			
C(b)–Fe–C(b′)	95.3(2)	Fe–C(b)–Fe′	82.0(2)
C(b)–Fe–C(t)	89.0(3)	C(b′)–Fe–C(t)	89.3(3)
C(b)–Fe–Cp	123.3	C(b′)–Fe–Cp	123.8
C(t)–Fe–Cp	126.0	Fe–C(t)–O(t)	177.2(7)
Fe–C(b)–O(b)	140.4(5)	Fe′–C(b)–O(b)	137.5(5)
C–C(11)–C(12)	127.5(4)	C(11)–C–C′	111.3(3)
C–C(11)–C(15)	124.0(4)	N–C–C′	111.2(3)
C(12)–C(11)–C(15)	107.6(4)	C(11)–C–N	110.2(4)
C(13)–C(12)–C(11)	108.4(5)	C(1)–N–C(1)	115.0(4)
C(14)–C(13)–C(12)	107.6(5)	C(1)–N–C(2)	112.5(4)
C(15)–C(14)–C(13)	108.0(5)	C(1)–N–C(2)	111.2(4)
C(11)–C(15)–C(14)	108.3(5)		

[a] Atoms labelled with a prime are related by the two-fold axis at $\frac{1}{4}$, y, $\frac{3}{8}$ and Cp represents the centroid of the cyclopentadienyl ring.

TABLE 11. Selected molecular dimensions with estimated standard deviations in parentheses of *R,R/S,S*-[$Fe_2\{\eta,\eta\text{-}C_5H_4CH(NMe_2)CH(NMe_2)C_5H_4\}(CO)_2(\mu\text{-}CO)_2$] (**2**) compared with those of its *R,S* isomer (**1**)

	S,S compound **2**	*R,S* compound **1** [1]	
Distances (Å)			
Fe(1)–Fe(2)	2.498(2)	2.510(1)	
Fe(n)–Cp(n)	1.734	1.729	1.743
Fe(1)–C(bn)	1.891(6)	1.932(8)	1.916(8)
Fe(2)–C(bn)	1.917(5)	1.926(8)	1.928(8)
Fe(n)–C(tn)	1.756(5)	1.770(9)	1.744(10)
C(bn)–O(bn)	1.193(5)	1.170(9)	1.177(9)
C(tn)–O(tn)	1.146(6)	1.128(11)	1.127(12)
Bond angles (°)			
C(b1)–Fe(n)–C(b2)	95.3(2)	96.6(3)	96.4(3)
Fe(1)–C(bn)–Fe(2)	82.0(2)	81.2(3)	81.5(3)
Fe(1)–C(bn)–O(bn)	140.4(6)	138.8(7)	139.0(7)
Fe(2)–C(bn)–O(bn)	137.5(5)	139.9(7)	139.5(6)
Dihedral angles (°)			
Fe(1),Fe(2),C(b1)–Fe(1),Fe(2),C(b2)	23.3	20.7	
C(b1),C(b2),Fe(1)–C(b1),C(b2),Fe(2)	26.2	23.6	

Cp(*n*) is the centroid cyclopentadienyl ring *n*.

reaction mixture, but the reaction of **1** with [$Fe(CO)_5$] does not give **3**.

3.1. Organic chemistry of 1 and 2

MeI or $MeOSO_2CF_3$ methylate (**1**) at N2 (Fig. 4) [14] and **2** at N1 to give [**4**]$^+$ and [**5**]$^+$ salts respectively. These will be described in detail elsewhere, but their organic chemistry allows the ring-linking two-carbon chain to be modified without affecting the $Fe_2(C_5H_4)_2(CO)_4$ moiety.

The reaction of [**4**]X with [$PhCH_2NMe_3$]OH in acetonitrile–methanol results in some demethylation to **1**, but the principal reaction is a Hofmann elimination of Me_3N and HX with formation of an enamine [$Fe_2\{\eta,\eta\text{-}C_5H_4CHC(NMe_2)C_5H_4\}(CO)_2(\mu\text{-}CO)_2$], (**6**)

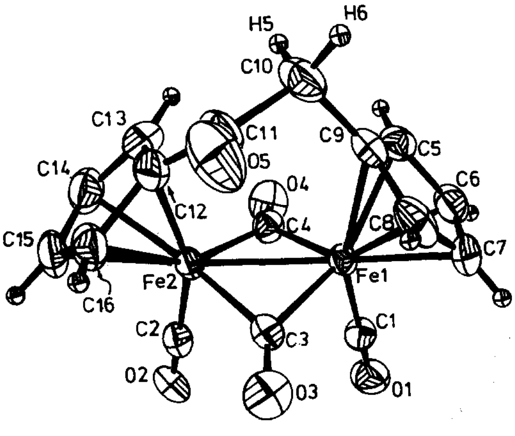

Fig. 3. The molecular structure and atom-labelling scheme for [$Fe_2\{\eta^5,\eta^5\text{-}C_5H_4CH_2C(O)C_5H_4\}(CO)_2(\mu\text{-}CO)_2$] (**8**).

TABLE 12. Fractional atomic coordinates for [$Fe_2\{\eta,\eta\text{-}C_5H_4CH_2C(O)C_5H_4\}(CO)_2(\mu\text{-}CO)_2$] with estimated standard deviations in parentheses

Atom	*x*	*y*	*z*
Fe(1)	0.05469(4)	0.14871(1)	0.13272(3)
Fe(2)	0.16218(4)	0.12123(1)	0.40077(3)
O(2)	−0.1290(3)	0.1741(1)	0.5533(2)
O(1)	−0.2816(3)	0.2150(1)	0.1651(2)
O(3)	−0.1257(3)	0.0448(1)	0.2486(2)
O(4)	0.2271(3)	0.2447(1)	0.3155(2)
O(5)	0.3477(4)	−0.0164(1)	0.1898(2)
C(1)	−0.1494(3)	0.1883(1)	0.1521(3)
C(2)	−0.0133(4)	0.1534(1)	0.4938(3)
C(3)	−0.0234(3)	0.0852(1)	0.2569(2)
C(4)	0.1753(3)	0.1958(1)	0.2925(3)
C(5)	0.2661(4)	0.1716(1)	−0.0038(3)
C(6)	0.0925(4)	0.1852(2)	−0.0762(3)
C(7)	−0.0102(5)	0.1312(2)	−0.0952(3)
C(8)	0.1057(5)	0.0849(1)	−0.0333(3)
C(9)	0.2773(4)	0.1098(1)	0.0260(3)
C(10)	0.4467(5)	0.0768(1)	0.0962(3)
C(11)	0.3912(4)	0.0353(1)	0.2168(3)
C(12)	0.3774(4)	0.0615(1)	0.3670(3)
C(13)	0.4542(4)	0.1161(1)	0.4254(3)
C(14)	0.3945(5)	0.1247(2)	0.5660(3)
C(15)	0.2810(5)	0.0757(2)	0.5947(3)
C(16)	0.2722(4)	0.0362(1)	0.4741(3)
H(1)	0.3577(39)	0.1996(12)	0.0238(29)
H(2)	0.0457(45)	0.2220(17)	−0.1026(37)
H(3)	−0.1222(47)	0.1254(12)	−0.1414(34)
H(4)	0.0876(39)	0.0485(13)	−0.0292(31)
H(5)	0.4906(45)	0.0488(15)	0.0116(36)
H(6)	0.5409(51)	0.1036(18)	0.1370(38)
H(7)	0.5331(49)	0.1431(14)	0.3779(37)
H(8)	0.4266(55)	0.1546(16)	0.6159(44)
H(9)	0.2220(42)	0.0697(14)	0.6773(35)
H(10)	0.2153(40)	0.0008(13)	0.4615(34)

TABLE 13. Bond lengths and angles for [$Fe_2\{\eta,\eta\text{-}C_5H_4CH_2C(O)C_5H_4\}(CO)_2(\mu\text{-}CO)_2$] with estimated standard deviations in parentheses

Bond lengths					
Fe(1)–Fe(2)	2.520(1)	Fe(1)–C(1)	1.751(3)		
Fe(1)–C(3)	1.929(2)	Fe(1)–C(4)	1.908(2)		
Fe(1)–C(5)	2.135(2)	Fe(1)–C(6)	2.093(2)		
Fe(1)–C(7)	2.084(3)	Fe(1)–C(8)	2.123(3)		
Fe(1)–C(9)	2.154(2)	Fe(2)–C(2)	1.756(3)		
Fe(2)–C(3)	1.932(2)	Fe(2)–C(4)	1.934(2)		
Fe(2)–C(12)	2.102(2)	Fe(2)–C(13)	2.110(3)		
Fe(2)–C(14)	2.116(3)	Fe(2)–C(15)	2.113(3)		
Fe(2)–C(16)	2.133(3)	O(2)–C(2)	1.144(3)		
O(1)–C(1)	1.147(3)	O(3)–C(3)	1.165(3)		
O(4)–C(4)	1.164(3)	O(5)–C(11)	1.211(4)		
C(5)–H(1)	0.93(3)	C(5)–C(6)	1.384(4)		
C(5)–C(9)	1.403(4)	C(6)–H(2)	0.91(4)		
C(6)–C(7)	1.418(5)	C(7)–H(3)	0.88(3)		
C(7)–C(8)	1.404(5)	C(8)–H(4)	0.82(3)		
C(8)–C(9)	1.411(4)	C(9)–C(10)	1.508(4)		
C(10)–H(5)	1.06(3)	C(19)–H(6)	0.95(4)		
C(10)–C(11)	1.515(4)	C(11)–C(12)	1.485(4)		
C(12)–C(13)	1.414(4)	C(12)–C(16)	1.414(4)		
C(13)–H(7)	0.96(3)	C(13)–C(14)	1.395(4)		
C(14)–H(8)	0.82(3)	C(14)–C(15)	1.409(5)		
C(15)–H(9)	0.91(3)	C(15)–C(16)	1.392(4)		
C(16)–H(10)	0.89(3)				
Bond angles					
C(1)–Fe(1)–Fe(2)	101.5(1)	C(2)–Fe(2)–Fe(1)	101.2(1)	Fe(1)–C(1)–O(1)	179.0(2)
C(3)–Fe(1)–C(1)	90.2(1)	C(3)–Fe(2)–C(2)	90.0(1)	Fe(1)–C(3)–O(3)	139.4(2)
C(4)–Fe(1)–C(1)	88.2(1)	C(4)–Fe(2)–C(2)	88.2(1)	Fe(1)–C(4)–O(4)	139.5(2)
C(4)–Fe(1)–C(3)	96.3(1)	C(4)–Fe(2)–C(3)	95.3(1)	Fe(1)–C(4)–Fe(2)	81.9(1)
C(5)–C(6)–C(7)	107.9(3)	C(12)–C(13)–C(14)	107.6(3)	Fe(1)–C(3)–Fe(2)	81.5(1)
C(6)–C(7)–C(8)	107.1(3)	C(13)–C(14)–C(15)	108.0(3)	Fe(2)–C(2)–O(2)	179.3(2)
C(7)–C(8)–C(9)	108.9(3)	C(14)–C(15)–C(16)	108.9(3)	Fe(2)–C(3)–O(3)	139.1(2)
C(8)–C(9)–C(5)	106.6(3)	C(15)–C(16)–C(12)	107.2(3)	Fe(2)–C(4)–O(4)	138.6(2)
C(9)–C(5)–C(6)	109.6(3)	C(16)–C(12)–C(13)	108.2(3)		
C(5)–C(9)–C(10)	125.8(3)	C(10)–C(11)–C(12)	117.4(3)		
C(8)–C(9)–C(10)	127.5(3)	C(10)–C(11)–O(5)	121.6(3)		
C(9)–C(10)–C(11)	109.0(2)	C(12)–C(11)–O(5)	120.9(3)		
H(5)–C(10)–C(11)	106 (2)	C(11)–C(12)–C(13)	127.7(3)		
H(6)–C(10)–C(11)	110 (2)	C(11)–C(12)–C(16)	124.0(3)		

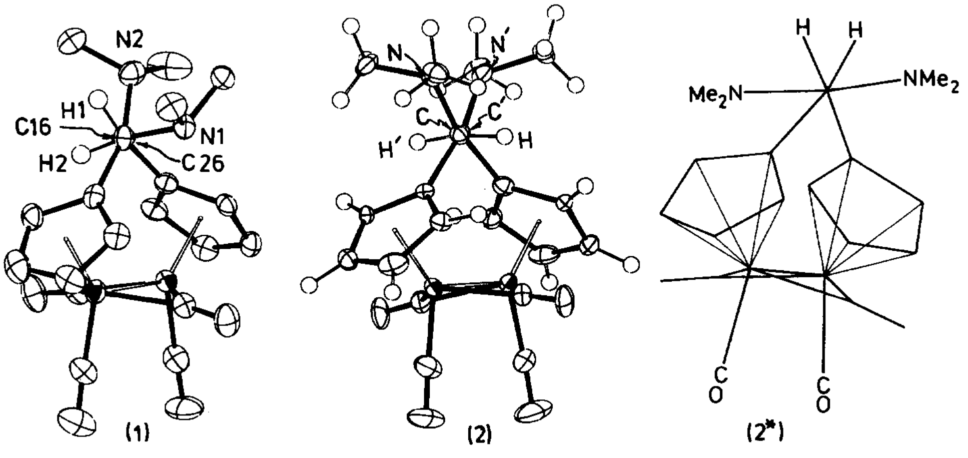

Fig. 4. The structures of **1** and **2** when viewed along the ring-linking C–C bond, and of the second unobserved form of **2**, namely **2** *.

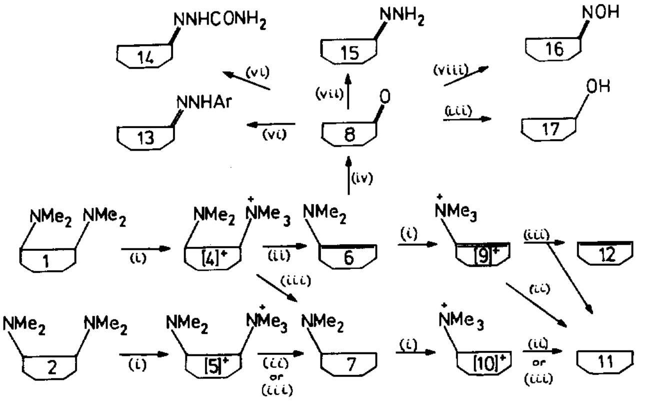

Scheme 1. $= [Fe_2(C_5H_4)_2(CO)_2(\mu\text{-}CO)_2]$; Ar = 2,4-$(NO_2)_2C_6H_3$. (i) $MeOSO_2CF_3$; (ii) $[PhCH_2NMe_3]OH$; (iii) $LiAlH_4$; (iv) H^+/H_2O; (v) 2,3-$(NO_2)_2C_6H_3NHNH_2 \cdot H_2SO_4$; (vi) $NH_2CONHNH_2 \cdot HCl/NaO_2CMe$; (vii) $NH_2NH_2 \cdot H_2O/MeCO_2H$; (viii) $NH_2OH \cdot HCl$.

with a moderate yield. In contrast, the reaction of [5]X with $[PhCH_2NMe_3]OH$ is much slower and gives a relatively low yield of the monoamine $[Fe_2\{\eta,\eta\text{-}C_5H_4CH_2CH(NMe_2)C_5H_4\}(CO)_2(\mu\text{-}CO)_2]$ (7) (see later).

A bimolecular E_2 mechanism [16] accounts for the above observations. The cation $[4]^+$ can assume an antiperiplanar arrangement of the two departing groups, H^+ and Me_3N, in a staggered rotamer of its observed structure (*i.e.* effectively alkylation at N1 in Fig. 4), and consequently undergo a relatively facile anti-elimination. Cation $[5]^+$ cannot assume an antiperiplanar configuration; consequently it can only undergo a *syn* elimination and to do so would have to adopt a *syn*-periplanar eclipsed conformation. As this would undoubtedly be of higher energy, the subsequent elimination would be much slower and in practice it is so slow that it does not compete effectively with the formation of **7** in the water gas shift reaction sequence shown in Scheme 2 ($Z = Me_2N$), which starts with attack by OH^- on the t-CO ligand of $[5]^+$ (*cf.* ref. 17) and ends with H^- displacement of Me_3N from another $[5]^+$. The higher yield of **7** in the presence of CO is readily explained (Scheme 2).

3.2. Reactions of the enamine $[Fe_2\{\eta,\eta\text{-}C_5H_4CHC(NMe_2)C_5H_4\}(CO)_2(\mu\text{-}CO)_2]$ (6)

The hydrolysis of **6** to the ketone $[Fe_2\{\eta,\eta\text{-}C_5H_4CH_2C(O)C_5H_4\}(CO)_2(\mu\text{-}CO)_2]$ (**8**), takes place on an alumina chromatography column but is best effected by stirring a solution of the enamine in acetonitrile with dilute aqueous hydrochloric acid.

Alkylation of the enamine **6** with $MeOSO_2CF_3$ gives $[Fe_2\{\eta,\eta\text{-}C_5H_4CHC(NMe_3)C_5H_4\}(CO)_2(\mu\text{-}CO)_2][SO_3CF_3]$, ([**9**][$SO_3CF_3$]). This salt does not undergo an N-to-C methyl migration, nor does **6** undergo a Stork reaction.

$$[Fe_2\{\eta,\eta\text{-}C_5H_4CH(Z)CH(NMe_3)C_5H_4\}(CO)_2(\mu\text{-}CO)_2]^+$$
$$\Big\downarrow +OH^-$$
$$[Fe_2\{\eta,\eta\text{-}C_5H_4CH(Z)CH(NMe_3)C_5H_4\}(CO_2H)(CO)(\mu\text{-}CO)_2]$$
$$\Big\downarrow -CO_2$$
$$[Fe_2\{\eta,\eta\text{-}C_5H_4CH(Z)CH(NMe_3)C_5H_4\}(H)(CO)(\mu\text{-}CO)_2]$$
$$\Big\downarrow \begin{array}{l} +[Fe_2\{\eta,\eta\text{-}C_5H_4CH(Z)CH(NMe_3)C_5H_4\}(CO)_2(\mu\text{-}CO)_2]^+ \\ -NMe_3 \end{array}$$
$$[Fe_2\{\eta,\eta\text{-}C_5H_4CH(Z)CH_2C_5H_4\}(CO)_2(\mu\text{-}CO)_2]$$
$$+$$
$$\text{“}[Fe_2\{\eta,\eta\text{-}C_5H_4CH(Z)CH(NMe_3)C_5H_4\}(CO)_3]^+\text{”}$$

Z = H or NMe_2 (*R*,*R*/*S*,*S*-isomer only)

Scheme 2.

3.3. Formation and reactions of the mono-amine $[Fe_2\{\eta,\eta\text{-}C_5H_4CH_2CH(NMe_2)C_5H_4\}(CO)_2(\mu\text{-}CO)_2]$ (7)

The reactions of [4]X or [5]X ($X^- = I^-$ or $SO_3CF_3^-$) with $LiAlH_4$ are exceptionally clean and facile. Those with $NaBH_4$ are much slower. In all cases, Me_3N is displaced by H^- and **7** is formed with a good yield. The reactions of [**4**][SO_3CF_3] and [**5**][SO_3CF_3] with $LiAlD_4$ give the same product, $[Fe_2\{\eta,\eta\text{-}C_5H_4CHDCH(NMe_2)C_5H_4\}(CO)_2(\mu\text{-}CO)_2]$ (**7-D**). The ^1H–^1H NMR coupling constants (Table 4) confirm unambiguously that **7** and **7-D** have the configuration shown

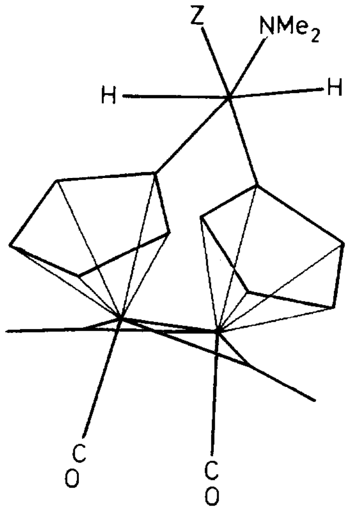

Fig. 5. The structure of 7 (Z = H) and 7-D (Z = D) when viewed along the ring-linking C–C bond.

in Fig. 5 [18]. The displacement of Me_3N by H^- from $[4]^+$ takes place with inversion of configuration at the relevant carbon atom, but that from $[5]^+$ with retention of configuration, perhaps via a common intermediate, such as a carbocation stabilized by internal $N \rightarrow C^+$ bonding which restricts attack by D^- at C^+ so that the only product is an $R,R'/S,S'$ and not an R,S' isomer.

Compound **7** can be alkylated by $MeOSO_2CF_3$ to give the salt $[Fe_2\{\eta,\eta\text{-}C_5H_4CH_2CH(NMe_3)C_5H_4\}(CO)_2(\mu\text{-}CO)_2][SO_3CF_3]$ ([**10**][SO_3CF_3]), which reacts with $LiAlH_4$ in carefully dried tetrahydrofuran to give the alkane $[Fe_2\{\eta,\eta\text{-}C_5H_4CH_2CH_2C_5H_4\}(CO)_2(\mu\text{-}CO)_2]$ (**11**). This is also the sole product from the reaction of [**10**][SO_3CF_3] with $[PhCH_2NMe_3]OH$, whereas a Hofmann elimination with formation of the alkene $[Fe_2\{\eta,\eta\text{-}C_5H_4CHCHC_5H_4\}(CO)_2(\mu\text{-}CO)_2]$ (**12**) would have been expected. Thus the elimination of Me_3N and H^+ from $[\mathbf{10}]^+$ is slow compared with the attack by OH^- on its terminal CO ligand (see above and Scheme 2). This implies that either an antiperiplanar configuration of H^+ and Me_3N in $[\mathbf{10}]^+$ can be achieved only with difficulty, or the presence of the NMe_2 group in $[\mathbf{4}]^+$ accelerates the elimination reaction which gives **6**, or both. An alternative route to (**12**), the reaction of [**9**][SO_3CF_3] with $LiAlH_4$, gave a 80% yield of a 1:3 mixture of **12** and **11** in which the components could not be separated but were identified by ^1H NMR spectroscopy. Compound **9** probably arises from the reduction of the initial product **12** by alane.

3.4. Reactions of the ketone $[Fe_2\{\eta,\eta\text{-}C_5H_4CH_2C(O)C_5H_4\}(CO)_2(\mu\text{-}CO)_2]$ (8)

As expected, **8** reacts with various RNH_2 to give a wide range of $[Fe_2\{\eta,\eta\text{-}C_5H_4CH_2C(NR)C_5H_4\}(CO)_2(\mu\text{-}CO)_2]$ derivatives containing the C=NR group where $R = NHC_6H_3(NO_2)_2\text{-}2,4$ (**13**), $NHCONH_2$ (**14**), NH_2 (**15**) or OH (**16**) (Table 2). The reduction of the ketone **8** with lithium aluminium hydride is fast in diethylether. The resultant secondary alcohol $[Fe_2\{\eta,\eta\text{-}C_5H_4CH_2CH(OH)C_5H_4\}(CO)_2(\mu\text{-}CO)_2]$ (**17**) was shown by ^1H NMR spectroscopy to have the same configuration as **7** (Fig. 5).

Surprisingly, **8** does not undergo the Mannich reaction with formaldehyde and amine hydrochloride salts under conditions in which aromatic ketones such as acetophenone react readily.

3.5. Infrared spectra

The infrared spectra of **1**, **2**, **2a**–**2c** and [**4**]X–(**17**) between 1750 and 2050 cm^{-1} (Table 3) are similar in the solid state and in solution, where they are independent of solvent. The pattern of absorption bands due to the $\nu(CO)$ vibrations are characteristic of *cis*-$[Fe_2(\eta^5\text{-dienyl})_2(CO)_2(\mu\text{-}CO)_2]$ complexes in which the $Fe_2(\mu\text{-}CO)_2$ moieties deviate slightly from planarity, and their assignment (Table 3) has been discussed in detail elsewhere [19]. The observed variations in frequencies are as expected. However, the spectra of some complexes also contain readily identified absorption bands due to the $\eta,\eta\text{-}C_5H_4\text{-}C\text{-}C\text{-}C_5H_4$ ligand (Table 3).

3.6. NMR spectra and fluxionality

The ^1H spectra and their assignment are summarized in Tables 4–6, and some ^{13}C spectra in Table 7. Coalescence temperatures T_c were used to calculate the activation energies ΔG_{T_c} (Table 8) for fluxional processes [20].

The spectra of **1**, **2**, **2a** and **2b** are all temperature dependent. In **1**, partial rotation about the ring-linking C–C bond (Fig. 4) is slowed at low temperatures so that the spectrum is then consistent with a R,S species with two inequivalent $Fe\{\eta^5\text{-}C_5H_4CH(NMe_2)\}(CO)$ moieties. This partial rotation does not appear to occur with **2**, **2a** and **2b**, as only one of the two possible $R,R/S,S$ isomers (Fig. 4) has been detected and is probably that found in the solid state for **2**. However, our data do not rule out the presence of both and their rapid interconversion even at 183 K. At low temperatures, rotation–inversion of one NMe_2 groups of **1** and both NR_2 groups of **2**, **2a** and **2b** can be slowed with ΔG_{T_c} increasing in the order **2** < **2a** < **2b**, perhaps owing to the increasing size of the NR_2 groups.

The ^{13}C NMR spectrum of $[Fe_2\{\eta,\eta\text{-}C_5H_4CH(NPhMe)CH(NPhMe)C_5H_4\}(CO)_2(\mu\text{-}CO)_2]$ (**2c**) (see below) suggests that it is an $R,R/S,S$ isomer. However, its ^1H NMR spectrum differs from that of **2** (or **1**), and is temperature dependent in all regions, owing probably to a single process. This may be a consequence of replacing NMe_2 by NMePh, with the expected downfield shift of the resonances due to the $C_5H_4CHN(Me)(R)CHN(Me)(R)C_5H_4$ moiety (*cf.* ref. 18), and the formation of additional chiral centres at N and additional enantiomorphs when rotation–inversion of the N(Me)Ph groups is slowed.

The assignment of the ^1H NMR spectra of **4**–**15** (Table 5) is straightforward. The spectra of **6**–**15** do not vary with temperature. This indicates that either **8** has a structure in solution where the two H atoms α to the keto group are equivalent or, more probably, it has the same structure in solution as in the solid state (see below), but with the two atoms undergoing rapid site exchange. Furthermore, unlike **1**, **2**, [**4**]X and [**5**]X, for which the interconversion of the methyl groups bound to nitrogen can be slowed on the NMR time scale, those of **6**, **7**, [**9**][SO_3CF_3] and [**10**][SO_3CF_3] cannot.

Comparison of the ^1H NMR spectrum of **3** (Table 6) with that of 6-dimethylaminofulvene [21] allows unambiguous assignment of the 7.33 ppm and 3.24 ppm resonances to the exocyclic proton H(12) and NMe_2 protons respectively (the numbering scheme is taken from ref. 3 and is shown in Fig. 1). Correlated double-resonance spectroscopy (NOESY) indicates that the protons that give rise to the following resonances are close together: 7.33, 6.13; 6.84, 3.24; 3.86, 2.78; 4.70, 3.92 ppm. This leads to the assignment shown in Table 5. Correlated double resonance spectroscopy (COSY) shows that there are numerous weak–proton couplings, but the only one of significance is that of 4.9 Hz between H9 and H10. The spectra of **3a** and **3b** are assigned similarly (Table 6).

On cooling of solutions of **3**, **3a** and **3b** the only significant changes are due to a slowing of the rotation of the planar NR_2 groups about the $C{-}NR_2$ bonds for which the activation energies ΔG_{T_c} (Table 8) increase for $R = Me$, $Et < {}^iPr$, probably because of greater crowding in **3b**. These compare with the value of 13.5 kcal mol^{-1} for 6-dimethylaminofulvene [22], which also has planar coordination about nitrogen atom and a multiple $C{-}NR_2$ bond.

3.7. ^{13}C NMR spectra

Those of **1** and **2** (Table 7) at 293 K are as expected. There is a single resonance due to the terminal CO ligands of **1**, **2**, **2a** and **2b**. However, **1** shows two resonances owing to its μ-CO ligands whilst **2**, **2a** and **2b** show only one, confirming that **2**, **2a** and **2b** are $R,R/S,S$ isomers with two equivalent μ-CO sites and **1** is an R,S isomer where they are different. On heating solutions of **1** in deuterochloroform the two μ resonances reversibly broaden and coalesce at *ca.* 378 K. The exchange of the two μ-CO ligands in a *cis*-$[Fe_2(\eta^5\text{-dienyl})_2(CO)_2(\mu\text{-}CO)_2]$ complex probably proceeds via an intermediate with four terminal (t) CO ligands and must be accompanied by μ–t CO exchange [22]. The ΔG_{T_c} for μ–μ and μ–t exchange of **1** is 15.6 kcal mol^{-1} compared with 11 ± 1.5 kcal mol^{-1} for $[Fe_2(\eta,\eta\text{-}C_5H_4CMe_2CMe_2C_5H_4)(CO)_2(\mu\text{-}CO)_2]$ [23]. The difference is probably due to steric effects if conversion one *gauche* non-bridged isomer to another also involves partial rotation about the ring-linking C–C bond.

The ^{13}C NMR spectra of **3** and **3b** are straightforward. However, in the case of **3a** there are four unequal components to the resonances at 37, 123 and 127 ppm, those at 71, 217 and 219 ppm are doublets, and there are four rather than two resonances between 108 and 103 ppm. This is inexplicable, as other spectroscopic data reveal no difference between **3** and **3a** or impurities in **3a**.

3.8. The structures of 2 and 8

X-ray diffraction studies confirm that **2** and **8** are closely related to that of *cis*-$[Fe(\eta^5\text{-}C_5H_5)_2(CO)_2(\mu\text{-}CO)_2]$ [24], $[Fe_2(C_{20}H_{16})(CO)_2((\mu\text{-}CO)_2]$ [23] and $[Fe_2\{C_{20}H_{16}Fe_2(CO)_6\}(CO)_2(\mu\text{-}CO)_2]$ [25] with similar dimensions and angles within their $Fe_2(C_5H_4)_2(CO)_2(\mu\text{-}CO)_2$ moieties. The data for **8** are of particularly high quality, with a very low R factor. Figures 2 and 3 show perspective drawings of the molecules together with atom-labelling schemes. The structure depicted for **2** has space-group-imposed molecular symmetry C_2, with an S conformation at each of the ring-linking carbon atoms C. However, in the crystal lattice, both S,S and R,R forms are present. Table 9 gives the molecular dimensions of **2** and in Table 10 some of these are compared with those for the previously reported R,S compound **1** [2]. In this latter compound the chiral carbon atoms C16 and C26 of the reported structure have the absolute configurations R and S respectively. Figure 4 depicts the structures of the S,S and R,S compounds when viewed along the ring-linking C–C bond. It shows that in the former the two H atoms are *transoid*, with a dihedral angle between them of 169° (Fig. 4), whereas in the latter they are *cisoid*, with a C_2H_2 dihedral angle of 78°, and also that in the former the cyclopentadienyl ring attached to C is shifted slightly, perhaps owing to packing factors.

The $C_5H_4C(O)$ moiety of **8** is virtually planar, indicating delocalization. The two CH_2 protons are inequivalent in the solid state although they undergo rapid interchange in solution even at 183 K (see above).

Acknowledgments

We thank Dr. W. Robinson of the University of Canterbury, New Zealand, for the collection of X-ray intensity data for **2**, and Irish Industrial Gases for a grant to M.G. Cox.

References

1 R.B. King and M.B. Bisnette, *Inorg. Chem.*, *3* (1964) 801.
2 F.S. Stephens, *J. Chem. Soc. A*, (1970) 1722.
3 U. Behrens and E. Weiss, *J. Organomet. Chem.*, *59* (1973) 335.
4 M.G. Cox, P. Soye and A.R. Manning, *J. Organomet. Chem.*, *369* (1989) C21.
5 K. Hafner, K.H. Vopel, G. Ploss and C. Konig, *Org. Synth. 47* (1967) 52.
6 H.T. Openshaw, *A Laboratory Manual of Qualitative Organic Analysis*, 2nd edn., Cambridge University Press, Cambridge, UK, 1951, p. 45.
7 *International Tables for X-ray Crystallography*, Kynoch, Birmingham, 1974, pp. 72–78 and 149.
8 C.K. Johnson, *ORTEP*, *Rep. ORNL-3794*, 1965, revised 1971. (Oak Ridge National Laboratory, TN.).
9 G.M. Sheldrick, *SHELX86*, *a Computer Program for Crystal Structure Determination*, University of Göttingen, Göttingen, 1986.
10 G.M. Sheldrick, *SHELX76*, *a Computer Program for Crystal Structure Determination*, University of Cambridge, Cambridge, UK, 1976.

11 D.T. Cromer and J.B. Mann, *Acta Crystallogr., Sect. A, 24* (1968) 321.

12 R.F. Stewart, E.R. Davidson and W.T. Simpson, *J. Chem. Phys., 42* (1965) 3175.

13 D.T. Cromer and D.J. Liberman, *J. Chem. Phys., 53* (1970) 1891.

14 P. McArdle and D. Cunningham, personal communication.

15 U. Behrens and E. Weiss, *J. Organomet. Chem., 96* (1975) 399.

16 J. Marsh, *Advanced Organic Chemistry*, 3rd edn., Wiley, New York, 1985, pp. 873–901.

17 P.C. Ford and A. Rokicki, *Adv. Organomet. Chem., 28* (1988) 139.

18 R.M. Silverstein, G.C. Bassler and T.C. Morrill, *Spectrometric Identification of Organic Compounds*, 4th edn., Wiley, New York, 1981.

19 A.R. Manning, *J. Chem. Soc. A,* (1968) 1319.

20 T.R. Jack and J. Powell, *Can. J. Chem., 53* (1975) 2558; H. Shanan-Atidi and K.H. Bar-Eli, *J. Phys. Chem., 74* (1970) 961.

21 J.H. Crabtree and D.J. Bertelli, *J. Am. Chem. Soc., 89* (1967) 5384; A.P. Downing, W.D. Ollis and I.O. Sutherland, *J. Chem. Soc. B,* (1969) 111.

22 R.D. Adams and F.A. Cotton, *J. Am. Chem. Soc., 95* (1973) 6589.

23 F.A. Cotton, D.L. Hunter, P. Lahuerta and A.J. White, *Inorg. Chem., 15* (1976) 557.

24 R.F. Bryan, P.T. Greene, M.J. Newlands and D.S. Field, *J. Chem. Soc. A.,* (1970) 3068.

25 M.R. Churchill and P.H. Bird, *Inorg. Chem., 8* (1969) 1941.